NASA TECHNICAL NOTE

NASA TN D-7772

NASA TN D-7772

ANALYSIS OF IMPINGEMENT HEAT TRANSFER FOR TWO PARALLEL LIQUID-METAL SLOT JETS

by Robert Siegel

Lewis Research Center

Cleveland, Ohio 44135

NATIONAL AERONAUTICS AND SPACE ADMINISTRATION • WASHINGTON, D. C. • SEPTEMBER 1974

1. Report No.	2. Government Accession No.	3. Recipient's Catalog No.
NASA TN D-7772		

4. Title and Subtitle	5. Report Date
ANALYSIS OF IMPINGEMENT HEAT TRANSFER FOR TWO PARALLEL LIQUID-METAL SLOT JETS	September 1974
	6. Performing Organization Code
7. Author(s)	8. Performing Organization Report No.
Robert Siegel	E-7906
	10. Work Unit No.
9. Performing Organization Name and Address	502-04
Lewis Research Center National Aeronautics and Space Administration Cleveland, Ohio 44135	11. Contract or Grant No.
	13. Type of Report and Period Covered
12. Sponsoring Agency Name and Address	Technical Note
National Aeronautics and Space Administration Washington, D.C. 20546	14. Sponsoring Agency Code

15. Supplementary Notes

16. Abstract

An analytical method is developed for determining heat transfer by impinging liquid-metal slot jets. The method involves mapping the jet flow region, which is bounded by free streamlines, into a potential plane where it becomes a uniform flow in a channel of constant width. The energy equation is transformed into potential plane coordinates and is solved in the channel flow region. Conformal mapping is then used to transform the solution back into the physical plane and obtain the desired heat-transfer characteristics. The analysis given here determines the heat-transfer characteristics for two parallel liquid-metal slot jets impinging normally against a uniformly heated flat plate. The liquid-metal assumptions are made that the jets are inviscid and that molecular conduction is dominating heat diffusion. Wall temperature distributions along the heated plate are obtained as a function of spacing between the jets and the jet Peclet number.

17. Key Words (Suggested by Author(s))	18. Distribution Statement
Conformal mapping; Impingement heat transfer; Jet heat transfer; Jet impingement; Liquid-metal heat transfer	Unclassified - unlimited Category 33

19. Security Classif. (of this report)	20. Security Classif. (of this page)	21. No. of Pages	22. Price*
Unclassified	Unclassified	40	$3.25

* For sale by the National Technical Information Service, Springfield, Virginia 22151

ANALYSIS OF IMPINGEMENT HEAT TRANSFER FOR TWO PARALLEL LIQUID-METAL SLOT JETS

by Robert Siegel

Lewis Research Center

SUMMARY

An effective means for providing local cooling of a heated surface is to impinge single or multiple jets of coolant at the location to be cooled. Liquid metals are very effective heat-transfer fluids so it is worthwhile considering the use of liquid-metal jets. In this report an analytical method is developed for analyzing heat transfer of impinging single or multiple two-dimensional liquid-metal jets. Results are obtained for two parallel liquid-metal slot jets impinging normally against a flat plate that is uniformly heated. Wall temperature distributions along the plate are obtained as a function of the spacing between the jets and the jet Peclet number. For the Peclet number range covered here, turbulence is small so that the large molecular conduction of the liquid metal is dominating the diffusion of heat. As a consequence of the low Prandtl number of liquid metals, the fluid is assumed inviscid. The solution is obtained by first mapping the jet region into a potential plane wherein it becomes a uniform flow in a channel of uniform width. The energy equation is transformed into potential plane coordinates and solved analytically in the simple channel geometry. Conformal mapping is then used to transform the solution back into the physical plane so that the temperature distribution along the impingement plate is obtained.

INTRODUCTION

A technique for localized cooling of a heated surface is to direct a single jet or multiple jets of coolant fluid against the surface. Liquid metals are very effective heat-transfer fluids and hence liquid-metal jet impingement may provide a useful technique for critical localized cooling applications. When multiple parallel jets are directed against a surface, there is an interaction which is a function of the spacing between adjacent jets. It is desired to know the heat-transfer characteristics along the impinge-

ment plate and in what manner these characteristics are influenced by the interaction of the jets with each other.

Liquid metals have very small Prandtl numbers so that the molecular diffusion of heat in them is much larger than the molecular diffusion of momentum. As a result, for a situation where the viscous and thermal boundary layers are developing simultaneously within the flow, the viscous boundary layers are much thinner than the thermal boundary layers. Because of this, the assumption is often made that the viscous-layer development can be neglected in heat-transfer computations, and this assumption will be used here. Then the velocity field within the jet region can be obtained by an inviscid free jet analysis. For two parallel impinging inviscid slot jets the flow field has been obtained by use of conformal mapping in reference 1.

The present analysis is an extension of that in reference 2 where the heat transfer for a single impinging slot jet was considered. The solution is obtained by first mapping the two-dimensional jet flow region into a potential plane. In this plane the flow region becomes a uniform flow in a channel with parallel walls. The convective energy equation and its boundary conditions are transformed into the potential plane. The problem is thereby reduced to a heat conduction type of solution for the temperature distribution in a slab of uniform thickness moving across a plane of distributed heat sources. Results are obtained by generalizing a solution in reference 3. After the solution is obtained for the temperatures along the boundary representing the heated wall in the potential plane, a conformal transformation is used to obtain the corresponding distribution in the physical plane. Results are given as a function of the spacing between the jets and the Peclet number of one of the incident jets.

SYMBOLS

A	parameter in mapping of jet flow
b	half-width of undisturbed incident jet
C_p	specific heat of fluid
F	temperature response to unit step in heat flux
h	local heat-transfer coefficient
h_n	dimensionless jet widths (n = 1 or 2)
k	thermal conductivity of fluid
m	integer
Nu	local Nusselt number, h2b/k

$\hat{n}$	unit normal vector
Pe	Peclet number, $\lvert v_\infty \rvert 2b/\alpha$
q_w	heat flux specified at wall
S	half spacing between centerlines of incident jets
T	dimensionless temperature, $tk/2bq_w$
t	temperature
$\bar{t}$	mixed mean convective fluid temperature
$\vec{U}$	dimensionless fluid velocity vector, $\vec{u}/\lvert v_\infty \rvert$
$\vec{u}$	fluid velocity vector
u, v	velocities in x and y directions
X, Y	dimensionless coordinates, x/2b, y/2b
x, y	rectangular coordinates along and normal to plate
x'	value of x equal to either x_D or 0
α	thermal diffusivity, $k/\rho C_p$
β	quantity related to A in jet mapping
η	dummy variable of integration
ξ	intermediate variable in jet mapping
ρ	fluid density
Φ	dimensionless potential, $\varphi/\lvert v_\infty \rvert 2b$
Φ_0	the value of Φ at X = 0, Y = 0
φ	potential function
Ψ	dimensionless stream function, $\psi/\lvert v_\infty \rvert 2b$
Ψ_1, Ψ_2	free streamlines
ψ	stream function
∇	gradient, $\hat{i}\frac{\partial}{\partial x} + \hat{j}\frac{\partial}{\partial y}$
$\tilde{\nabla}$	dimensionless gradient, $2b\nabla$

Subscripts:

D	end of dividing streamline
s	at free streamline

w at wall

∞ undisturbed fluid condition

ANALYSIS

The analysis here is an extension of that in reference 2. For ease in following the present development some of the details in reference 2 will be repeated with the necessary modifications for the present situation.

Geometry

The geometric configuration is shown in figure 1 and consists of a pair of two-dimensional slot jets impinging against a plate that is uniformly heated. The undisturbed incident jets have their centerlines spaced 2S apart, and the width of each jet is 2b. The flow is inviscid and irrotational, and hence the flow configuration can be obtained by conformal mapping. This has been done in reference 1 and specific flow patterns will be given later.

After impingement, each jet turns so that for the two jet system being analyzed, there is a symmetric flow outward along the impingement plate in the positive and negative x directions. The portions of the turned flow going toward the y-axis between the jets form a recirculating jet that moves upward along the y-axis.

When the jets are sufficiently separated so that they do not appreciably influence each other, the flow moving outward toward larger positive and negative x has an asymptotic height equal to one-half the width of one of the incident jets. The recirculating jet moving upward along the y-axis has an asymptotic width equal to the width of one of the incident jets.

As the jets are moved closer to each other, that is S/2b is decreased, the width of the recirculating jet is decreased and the portions of the flow moving outward (away from the y-axis) are increased. As the spacing between the jet centerlines approaches the incident jet width (2S = 2b), the recirculating jet decreases to zero and the two incident jets merge to form a single incident jet of width 4b.

Governing Equations

When a flow moves along a heated plate, there is a development of both thermal and hydrodynamic boundary layers. Liquid metals, which are being considered here, have

very low Prandtl numbers (in the range 0.005 to 0.02) indicating that thermal diffusion is much larger than viscous diffusion. Hence, the thermal boundary layers will be thick compared with the viscous regions and to a good approximation the flow can be considered inviscid when computing the heat-transfer characteristics. It is also assumed that the jet Reynolds number is low enough so that turbulent diffusion of heat can be neglected compared with the large molecular diffusion of heat characteristic of a liquid metal.

For inviscid irrotational flow the fluid velocity is equal to the gradient of a potential,

$$\vec{u} = \nabla\varphi \tag{1}$$

The Cauchy-Riemann equations apply, and these relate the velocity potential to the stream function,

$$u = \frac{\partial\varphi}{\partial x} = \frac{\partial\psi}{\partial y} \tag{2a}$$

$$v = \frac{\partial\varphi}{\partial y} = -\frac{\partial\psi}{\partial x} \tag{2b}$$

Then from the continuity equation $\partial u/\partial x + \partial v/\partial y = 0$, and by substituting equations (2) for u and v, the velocity potential satisfies Laplace's equation, $\nabla^2\varphi = 0$. Equating $\frac{\partial}{\partial y}\left(\frac{\partial\varphi}{\partial x}\right)$ from equation (2a) to $\frac{\partial}{\partial x}\left(\frac{\partial\varphi}{\partial y}\right)$ from equation (2b) shows that ψ also satisfies the Laplace equation, $\nabla^2\psi = 0$.

The energy equation for the flow consists of a convection term and a conduction term,

$$\rho C_p \vec{u} \cdot \nabla t = k \nabla^2 t \tag{3}$$

By substituting equation (1) this becomes

$$\rho C_p \nabla\varphi \cdot \nabla t = k \nabla^2 t \tag{4}$$

Boundary Conditions

Since the flow solution is already available in reference 1, it is not necessary to consider the flow boundary conditions, and it is only the thermal boundary conditions that are of interest here. All of the flow and thermal conditions are symmetric about

the y-axis so it is necessary to only consider the region where x is positive as shown in figure 2. The symmetry about the axis $\widehat{67}$ yields

$$\frac{\partial t}{\partial x} = 0 \qquad x = 0,\ y \geq 0 \tag{5}$$

It is assumed that along the free streamlines there are negligible heat losses compared with the energy convected by the flow so that

$$\hat{n}_s \cdot \nabla t = 0 \qquad x, y \text{ on } \widehat{12} \text{ and } \widehat{45} \tag{6}$$

Along the impingement plate there is an imposed uniform heat flux q_w so that,

$$\frac{\partial t}{\partial y} = -\frac{q_w}{k} \qquad 0 \leq x \leq \infty,\ y = 0 \tag{7}$$

Along the cross section of the incoming undisturbed jets the fluid is at a uniform temperature t_∞,

$$t = t_\infty \qquad x, y \text{ on } \widehat{24} \tag{8}$$

Equations and Boundary Conditions in Dimensionless Form

The following dimensionless variables are used:

$$\left.\begin{aligned} X &= \frac{x}{2b} & Y &= \frac{y}{2b} \\ \tilde{\nabla} &= 2b\nabla & \vec{U} &= \frac{\vec{u}}{|v_\infty|} \\ \Phi &= \frac{\varphi}{|v_\infty| 2b} & \Psi &= \frac{\psi}{|v_\infty| 2b} \\ T &= \frac{tk}{2bq_w} & Pe &= \frac{|v_\infty| 2b}{\alpha} \end{aligned}\right\} \tag{9}$$

The velocity and energy equations (1) and (4) then become

$$\vec{U} = \tilde{\nabla}\Phi \tag{10}$$

$$Pe\ \tilde{\nabla}\Phi \cdot \tilde{\nabla}T = \tilde{\nabla}^2 T \tag{11}$$

The boundary condition equations (5), (6), (7), and (8) become

$$\frac{\partial T}{\partial X} = 0 \qquad X = 0,\ Y \geq 0\ (X, Y \text{ on } \widehat{67}) \tag{12}$$

$$\hat{n}_s \cdot \tilde{\nabla}T = 0 \qquad X, Y \text{ on } \widehat{12} \text{ and } \widehat{45} \tag{13}$$

$$\frac{\partial T}{\partial Y} = -1 \qquad 0 \leq X \leq \infty,\ Y = 0 \qquad (X, Y \text{ on } \widehat{79}) \tag{14}$$

$$T = T_\infty \qquad X, Y \text{ on } \widehat{24} \tag{15}$$

Solution of the Flow Problem

The inviscid irrotational impinging jet configuration in figure 1 has been analyzed by conformal mapping in reference 1. In figure 2 one-half the symmetric configuration is shown with various points numbered. The mapping into the potential plane is shown in figure 3. In figure 3 (and in the equations that follow) there is a parameter A that occurs in the conformal mapping solution and is related to the dimensionless spacing between the jet centerlines. The location of point 7 in figures 2 and 3 depends on whether A is positive or negative; for the former, X_D is on the heated plate and for the latter it is on the symmetry line (Y-axis). The nature of the flow (and its relation to A) is better understood by examining the streamline configurations in figure 4. In figure 4(a) the jet centerlines are spaced 4.42 slot widths apart and the stagnation point where the dividing streamline of each jet strikes the plate is only very slightly closer to the y-axis in comparison with the centerline of that jet; this corresponds to $A = 0.9$. For infinite spacing between the jets ($A \to 1$) the flow from each jet divides equally to the right and left which is approximately the situation for the spacing in figure 4(a). From symmetry there is a second stagnation point on the plate at $X = 0$.

A decrease in spacing between the jets causes the stagnation point where the dividing streamline strikes the plate to shift toward $X = 0$, and in figure 4(b), 60 percent of the flow is turned toward the right. When the spacing $S/2b = 1.38$ ($A = 0$), the stag-

nation point at the end of the dividing streamline has shifted to the origin (fig. 4(c)). A further decrease in spacing as shown in figure 4(d) ($A < 0$) causes the end of the dividing streamline to move upward along the Y-axis, and there is still a stagnation point on the plate at $X = 0$. In figure 4(e) ($A = -1.0$), the spacing between the jets has been reduced to the extent that a single jet has been formed.

The mapping of the flow from the physical plane into the potential plane, as given in reference 1, yields the configuration in figure 3 which is a parallel plate channel with a uniform flow moving from left to right. The upper and lower boundaries of the channel correspond to the jet free streamlines. The dividing streamline $\widehat{38}$ is not in the center of the channel as there are unequal flows on either side of this streamline in the physical geometry. The folded line $\widehat{689}$ is the streamline consisting of the heated plate and the y-axis. The heated plate $\widehat{79}$ occupies a different location in figures 3(a) and (b) depending on whether the dividing streamline terminates at the plate or at the Y-axis as discussed in relation to figure 4.

The flow quantities that are needed in the heat-transfer solution are the velocity along the heated plate, and the correspondence between the potential Φ along the plate and the physical X coordinate. From reference 1 the velocity in the X direction along the plate is given by the following expression in terms of the parameter A and an intermediate variable ξ that is related to X (as will be given by eq. (18)),

$$U = \frac{u}{|v_\infty|} = \frac{\xi^{1/2}(\xi - A)}{1 - \xi A} \qquad 0 \le \xi \le 1 \tag{16}$$

As indicated in figure 4 and discussed previously, the parameter A is related to the spacing between the jet centerlines; the relation is given by

$$\frac{S}{2b} = \frac{A + 3}{4} + \frac{3 - A}{4\pi} \ln\left[\frac{1 + \cos(\beta/2)}{1 - \cos(\beta/2)}\right] \tag{17}$$

where

$$\beta = \cos^{-1}\left(\frac{-A^2 + 2A + 1}{2}\right)$$

Along the heated plate the ξ is related to X and Φ by

$$X = \frac{2}{\pi}\tan^{-1}\left[\frac{(1 - A)\xi^{1/2}}{1 - \xi}\right] + \frac{3 - A}{2\pi}\ln\left(\frac{1 + \xi^{1/2}}{1 - \xi^{1/2}}\right) + \frac{(A + 1)}{\pi}\tan^{-1}\xi^{1/2} \tag{18}$$

$$\Phi = -\frac{(3 - A)}{2\pi} \ln\left|\frac{1 - \xi}{1 - A}\right| - \frac{A + 1}{2\pi} \ln\left|\frac{\xi + 1}{A + 1}\right| + \frac{1}{\pi} \ln\left|\frac{\xi^2 + \xi(A^2 - 2A - 1) + 1}{A^2 + A(A^2 - 2A - 1) + 1}\right| \tag{19}$$

For the positive values of A there are two ranges of variables in the equations relating Φ, ξ, and X depending on whether the location being considered along the impingement plate is to the left or to the right of the stagnation point X_D at the end of the dividing streamline as shown in figure 2,

$$0 \leq X \leq X_D \qquad 0 \leq \Phi \leq \Phi(\xi=0) \qquad 0 \leq \xi \leq A \tag{20}$$

$$X_D \leq X \leq \infty \qquad 0 \leq \Phi \leq \infty \qquad A \leq \xi \leq 1 \tag{21}$$

From the mapping relations, the X_D is found from equation (18) by letting $\xi = A$. For negative A the X_D is zero and there is only one range

$$0 \leq X \leq \infty \qquad \Phi(\xi=0) \leq \Phi \leq \infty \qquad 0 \leq \xi \leq 1 \tag{22}$$

Formulation for Heat-Transfer Solution by Means of Potential Plane

The channel type of region in figure 3 offers a convenient geometry in which to solve the energy equation. The energy equation (11) has the same form as equation (16) in reference 4. The details of the transformation of the energy equation from the physical plane (X, Y coordinates) to the potential plane (Φ, Ψ coordinates) are given in reference 4 and there is no need to repeat them here. Using equation (26) of reference 4 yields the energy equation as

$$\frac{\partial^2 T}{\partial \Phi^2} + \frac{\partial^2 T}{\partial \Psi^2} - Pe \frac{\partial T}{\partial \Phi} = 0 \tag{23}$$

This is the same equation as for forced convection heat transfer to a uniform flow in a parallel plate channel. The flow in the channel is in the Φ direction so the $\partial^2 T/\partial \Phi^2$ corresponds to the axial conduction term. This term is usually small compared with the Pe $\partial T/\partial \Phi$ term which corresponds to axial convection.

In reference 2 solutions were obtained for impingement heat transfer of a single jet with and without the $\partial^2 T/\partial \Phi^2$ term included. For $Pe > 20$ the two solutions differed negligibly. For $Pe = 10$ there was a few percent error when $\partial^2 T/\partial \Phi^2$ was neglected, and for $Pe = 5$ the error was several percent. Hence, in most instances it is reason-

able to neglect the $\partial^2 T/\partial \Phi^2$ term; this will offer considerable simplification for the present situation which is geometrically more complex than that in reference 2. The solution will break down in the vicinity of $x = 0$ for large spacings between the jets where there is a back flow region around $x = 0$. In this type of flow region the simplified solution will lead to a zero convective heat-transfer coefficient, whereas including the term $\partial^2 T/\partial \Phi^2$ would cause the heat transfer to be finite. This type of analytical prediction is analogous to the infinite heat-transfer coefficient calculated at the entrance of a heated channel as a result of neglecting axial conduction. With $\partial^2 T/\partial \Phi^2$ neglected, the energy equation (23) that is to be solved reduces to

$$\frac{\partial^2 T}{\partial \Psi^2} = Pe \frac{\partial T}{\partial \Phi} \tag{24}$$

This equation has the same form as the transient heat conduction equation.

To solve equation (24), the thermal boundary conditions equations (12) to (15) must also be transformed into the potential plane. The symmetry condition equation (12) becomes

$$\frac{\partial T}{\partial \Psi} = 0 \qquad \Phi, \Psi \text{ on } \widehat{67} \tag{25}$$

The free streamlines $\widehat{12}$ and $\widehat{45}$ are lines of constant Ψ so that the condition equation (13) becomes

$$\frac{\partial T}{\partial \Psi} = 0 \qquad \Phi, \Psi \text{ on } \widehat{12} \text{ and } \widehat{45} \tag{26}$$

To transform equation (14), the relation is used that at a fixed X

$$\frac{\partial T}{\partial Y} = \frac{\partial T}{\partial \Psi}\frac{\partial \Psi}{\partial Y} + \frac{\partial T}{\partial \Phi}\frac{\partial \Phi}{\partial Y}$$

Since $\partial \Phi/\partial Y$ is the V velocity component which is zero along the heated plate, this relation becomes the following with the aid of equation (14) along the plate:

$$-1 = \frac{\partial T}{\partial \Psi}\frac{\partial \Psi}{\partial Y} \qquad \Phi, \Psi \text{ on } \widehat{79}$$

From equation (2a) $\partial\Psi/\partial Y = U$ so the boundary condition further reduces to

$$\frac{\partial T}{\partial \Psi} = -\frac{1}{U(\Phi)} \qquad \Phi, \Psi \text{ on } \widehat{79} \tag{27}$$

The $U(\Phi)$ is obtained from equations (16) and (19). The final boundary condition (15) becomes

$$T = T_\infty \qquad \Phi, \Psi \text{ on } \widehat{24} \tag{28}$$

The boundary conditions are summarized in figure 3 for the two possible situations where the dividing streamline terminates at either the heated plate or along the y-axis.

Solution for Temperature Distribution Along Heated Plate

In the potential plane the flow becomes a channel flow with a uniform velocity throughout as shown in figure 3; this will be called a moving slab to distinguish it from the flow in the physical plane. The dividing streamline $\widehat{38}$ and the mapping of boundary $\widehat{69}$ divide the channel into two portions with widths h_1 and h_2. From the mapping solution in reference 1 these are given by

$$h_1 = \frac{1}{2} - \frac{1 - A}{4} \tag{29a}$$

$$h_2 = \frac{1}{2} + \frac{1 - A}{4} \tag{29b}$$

where it is recalled from equation (17) that A is only a function of the dimensionless spacing between the jet centerlines. The upper and lower boundaries of the entire channel are insulated. With axial conduction neglected there is no propagation of energy in the negative Φ direction and as a consequence the moving slab is not heated until it reaches the most leftward portion of the heated area $\widehat{79}$ as mapped into the potential plane. As a result of the coordinate transformation, the uniform heat addition along $\widehat{79}$ in the physical plane becomes a nonuniform heat source distribution along the corresponding area in the potential plane. Since the flow velocity is uniform in the potential plane, the flow in each of the portions of the channel of width h_1 or h_2 is a solid slab moving past a nonuniform heat source along one boundary.

In the physical plane the problem is one of uniform heat transfer into a fluid with

nonuniform velocity; under transformation to the potential plane this becomes a problem with a nonuniform heat transfer to a uniform (slab) flow. The solution is already available for this latter situation. If we take the viewpoint of an observer at a fixed axial location on the slab, then the slab appears stationary with a heat flux at the surface at that axial location that is varying with time. Thus because equation (24) has the same form as the transient heat conduction equation, the solution is the same as for a slab of thickness h_1 or h_2 that is initially at uniform temperature, has one boundary that is kept insulated, and has on the other boundary a heat input that varies with time. The solution can be found by using a superposition in time of the uniform heat flux solution in equation (4) on page 112 of reference 3. The details of the derivation are in appendix A, and the solution for the wall temperature along the heated plate is as follows:

For spacings between jets such that the dividing streamline ends on the heated plate, $S/2b > 1.38$ $(0 < A \leq 1)$, the $T_w(\Phi)$ is found from

$$\frac{(t_w - t_\infty)k}{2bq_w} = T_w(\Phi) - T_\infty = \frac{1}{\sqrt{\pi\,Pe}} \int_0^\Phi \frac{1}{\eta^{1/2}\left|U(\Phi - \eta)\right|} \times \sum_{m=0}^{\infty} \left[e^{-m^2 Peh_n^2/\eta} + e^{-(m+1)^2 Peh_n^2/\eta} \right] d\eta \qquad (30)$$

There are two ranges corresponding to X values on either side of the stagnation point X_D in figure 2.

For

$$0 \leq X \leq X_D, \qquad h_n = h_1 = \frac{1}{2} - \frac{1 - A}{4}$$

$$X_D \leq X \leq \infty, \qquad h_n = h_2 = \frac{1}{2} + \frac{1 - A}{4}$$

To obtain $\left|U(\Phi)\right|$ for any argument Φ, it is necessary to first obtain ξ at that Φ. From the flow mapping, the ξ is double valued for part of the Φ range,

$$\text{for } 0 \leq X \leq X_D\text{: } 0 \leq \xi \leq A \qquad 0 \leq \Phi \leq \Phi_0$$

$$\text{for } X_D \leq X \leq \infty\text{: } A \leq \xi \leq 1 \qquad 0 \leq \Phi \leq \infty$$

where Φ_0 is found by letting $\xi = 0$ in equation (19). The U is evaluated from equation (16).

For spacings between jets such that the dividing streamline ends on the plane of symmetry between the jets $S/2b < 1.38$ $(-1 \leq A < 0)$, the $T_w(\Phi)$ is found from

$$\frac{(t_w - t_\infty)k}{2bq_w} = T_w(\Phi) - T_\infty = \frac{1}{\sqrt{\pi\,Pe}} \int_0^{\Phi - \Phi_0} \frac{1}{\eta^{1/2} U(\Phi - \eta)} \times \sum_{m=0}^{\infty} \left[e^{-m^2 Peh_2^2/\eta} + e^{-(m+1)^2 Peh_2^2/\eta} \right] d\eta \qquad (31)$$

There is only one range,

$$0 \leq X \leq \infty: \quad 0 \leq \xi \leq 1 \qquad \Phi_0 \leq \Phi \leq \infty$$

This is because in this instance, as shown by figure 3(b), the heated boundary $\widehat{79}$ is in contact with only one portion of the moving slab (the portion having width h_2).

For a given value of the jet spacing $S/2b$ the parameter A is found from equation (17). Then for a given X value, the corresponding Φ to be used in equations (30) and (31) is found from equations (18) and (19).

As X approaches zero (which corresponds to Φ approaching Φ_0) equation (31) can be evaluated analytically. The analysis is given in appendix B with the result

$$T_w(X \to 0) - T_\infty = \left(\frac{A - 3}{A\,Pe} \right)^{1/2} \qquad S/2b < 1.38 \qquad (-1 \leq A < 0) \qquad (32)$$

For large X the flow has turned along the plate, and for the inviscid solution the velocity becomes uniform and equal to v_∞ (fig. 5). The heat-transfer situation at large X consists of a channel flow with the lower boundary being a flat plate with uniform heat addition. The upper boundary is a free streamline which is assumed to act as an insulated boundary. This situation is analyzed in appendix C and the result for the wall temperature at large X is

$$T_w - T_\infty = \frac{X - X_D}{Pe\,h_2} + \frac{h_2}{3} \qquad \frac{S}{2b} \geq 1.38 \qquad (33a)$$

$$T_w - T_\infty = \frac{X}{Pe\, h_2} + \frac{h_2}{3} \qquad \frac{S}{2b} \le 1.38 \tag{33b}$$

Results from these relations are shown in figure 6. As X increases, this limiting solution can approach the actual solution from above or below. The limiting solution is for a uniform velocity distribution and a fully developed temperature distribution. The nature of the asymptotic approach at large X then depends on the relative rates at which the velocity distribution approaches uniform flow and the thermal boundary layer development becomes a fully developed distribution. This is a function of the Peclet number on which the thermal boundary layer growth depends.

DISCUSSION

For spacings between the jets such that the dividing streamline ends at the heated plate ($S/2b > 1.38$), equation (30) was used to calculate the temperature distribution along the impingement plate, and results for various values of the Peclet number are given in figures 6(a) to (c). For close spacings ($S/2b < 1.38$), equations (31) and (32) were used to obtain the results in figures 6(d) to (g). The condition analyzed here is for the impingement plate being uniformly heated and hence it is the wall temperature distribution that is of interest. The results on the figures can also be expressed in terms of a heat-transfer coefficient or Nusselt number. The local heat-transfer coefficient along the plate is $h = q_w/(t_w - t_\infty)$ or $h = \left[2bq_w/(t_w - t_\infty)k\right](k/2b)$. Hence the local h is k/2b divided by the ordinate of the curves. If the Nusselt number is defined as $Nu = h2b/k$, then the local Nusselt number is the reciprocal of the ordinate in figure 6.

From symmetry only half of the flow configuration need be considered, so this discussion will be concerned with the positive X region only. Also from symmetry there is no flow of fluid or heat across the Y-axis, so this axis can be regarded as a solid wall that is perfectly insulated; thus the results also apply to the case of an inviscid jet impinging on a heated wall that is adjacent to a 90° corner formed with an insulated wall.

In figure 6(a) the jets are spaced fairly far apart, $S/2b = 2.5$, so that the flow configuration is similar to that in figure 4(a). The jet divides about equally to the right and left, and as shown in figure 6(a) the stagnation point X_D at the end of the dividing streamline is close to the centerline of the incident jet. For comparison, curves are given for a single jet impinging on an infinite plate as analyzed in reference 2 (the results taken from ref. 2 are for the case with axial conduction neglected as in the present case). At the stagnation point and to the right of the stagnation point the results for the present case are essentially like that for a single jet. The flow to the left, however, is interfered with by the flow moving toward the Y-axis from the symmetrically placed jet

at negative X. The turning of the flow away from the plate reduces the ability of the flow to transfer heat in this region which results in an increase in local wall temperature. Also shown on the figure are the results for large X as predicted by equation (33). These results agree quite well with the curves when X is greater than about 5. For the inviscid approximation, and as is typical for liquid metals, the results depend on the Peclet number ($|v_\infty| 2b/\alpha$) which is independent of viscosity. This dependence shows that an increase in, for example, the flow velocity increases the Peclet number and is associated with lower wall temperatures and improved heat transfer.

Figures 6(b) and (c) show wall temperature curves similar to those in figure 6(a) except for decreased spacings of $S/2b = 2$ and 1.5. For both of these spacings the stagnation point at the end of the dividing streamline is along the heated plate and part of the energy is being convected away to the left and then upward along the Y-axis. This provides poor heat transfer at small X values. The singularity at $X = 0$ results from the neglect of axial conduction; this is the same type of singularity that provides an infinite heat-transfer coefficient at the origin of a developing thermal boundary layer.

In figure 6(d) the spacing has been decreased such that $S/2b = 1.25$. This spacing is less than the value $S/2b = 1.38$ at which there is a shift in the end point of the dividing streamline from being on the heated plate to being on the Y-axis. Now all the energy is being convected away by the flow to the right, and at $X = 0$ the flow is toward the plate. At $X = 0$ there is a stagnation point for incident flow rather than a stagnation point for flow moving away from the plate which was the situation for $S/2b > 1.38$. For each Peclet number the wall temperature then approaches a finite value as $X \to 0$ as is typical for an impinging jet stagnation region. From figures 4(c) and (d) it is noted that near $X = 0$ there is a large spacing between the heated plate and the adjacent streamline so that there is a low velocity region near $X = 0$ for $S/2b$ between 1.38 and 1.00. The resulting poor heat transfer causes the wall temperature to be high in the region of $X = 0$ as shown in figure 6(d).

As $S/2b$ is further decreased, the two jets begin to merge into one. In figures 6(e) and (f) the peak temperature at $X = 0$ diminishes as $S/2b$ decreases. Figure 6(g) gives the limiting case of $S/2b = 0.5$ for which the two impinging jets have merged into a single impinging jet of width $4b$ as shown in figure 4(e). The results approach the single jet solution in reference 2 as $S/2b$ approaches 0.5.

To better examine the effect of spacing between the impinging jets, the results are given in figure 7 for the fixed Peclet numbers 5 and 20 and for various spacings at each Peclet number. To follow the trends of a typical set of curves on either figure 7(a) or (b), start with the curve for $S/2b = 0.5$ which corresponds to the two jets being merged into a single jet. When $S/2b$ is increased to 0.75, part of the flow is recirculated upward along the y-axis, but since the dividing streamline terminates along the y-axis, none of this recirculating flow moves along the heated plate. Hence, increasing the

spacing in this range serves only to direct some of the flow from the plate which reduces the heat-transfer ability and raises the wall temperature curve. This trend continues as $S/2b$ is further increased until $S/2b$ exceeds 1.38. For any larger spacings the dividing streamline terminates at the impingement plate and both portions of the flow go along the plate. The fluid is thus utilized more efficiently for convective heat transfer and the plate temperatures are decreased. This trend continues as the spacing is further increased and the two impinging jets interfere less with each other. When $S/2b$ is greater than about 2.5, the two jets are acting independently except for the region near the y-axis where the flows collide and form an upward flow along the y-axis.

CONCLUSIONS

An analytical method has been devised for determining the heat-transfer behavior of impinging two-dimensional liquid-metal jets. The method combines free jet theory and a transformation of the energy equation into the potential plane. In the potential plane the transformed jet flow region occupies a parallel plate channel. The energy equation is solved in this geometrically convenient region, and the resulting temperature distributions along the heated plate are then transformed into the physical plane. To demonstrate the method, the heat-transfer behavior has been analyzed for two parallel slot jets impinging on a uniformly heated wall. The analysis can also be used for a nonuniformly heated wall as this only requires the heat source distribution to be changed in equations (30) and (31).

When the jets impinge on the plate, the flow from each of them divides with one portion flowing along the plate away from both of the jets, and the other portion flowing toward the centerplane between the jets. The latter portions collide and recirculate in the region between the jets. The half spacing between the centerlines of the incident jets is S and the width of each incident jet is $2b$. When the spacing between the jets is small, $S/2b < 1.38$, a portion of the flow recirculates between the jets without flowing along the heated plate. This decreases the effectiveness of the impingement heat transfer.

As $S/2b$ is increased beyond 1.38 the interference of the jets is reduced and the flow on either side of each jet stagnation point flows along the heated plate. Each jet begins to act more as an isolated jet with the impingement region heat transfer improving as the spacing is increased (i.e., as the mutual interference of the jets is further

decreased). When S/2b is increased to approximately 2.5, the stagnation region heat transfer has increased to that for an isolated jet.

Lewis Research Center,
National Aeronautics and Space Administration,
Cleveland, Ohio, May 26, 1974,
502-04.

APPENDIX A

SOLUTION OF ENERGY EQUATION

The analysis showed that the energy equation in the potential plane was reduced to an equation in the same form as the one-dimensional transient heat conduction equation (eq. (24)). The Φ in the present analysis is analogous to time in the corresponding transient problem. Since the heating along the boundary $\widehat{79}$ varies with Φ as shown in figure 3, the problem is equivalent to transient heat conduction with time variable heating at the boundary. The other boundary of the heated region, that is either $\widehat{12}$ or $\widehat{45}$ in figure 3, is insulated. In reference 3 (p. 112), the transient solution is given for a heat flux suddenly applied at time zero at one surface of a slab with the other surface of the slab insulated. Let the wall temperature response (relative to the initial fluid temperature T_∞) to a unit heat flux be called F. Then by superposition, since the energy equation is linear, the response to an applied variable flux $\partial T/\partial \Psi(\Phi)$ can be obtained. The superposition integral is obtained from reference 5 (p. 404) by a change in variable as,

$$T_w(\Phi) - T_\infty = \int_0^\Phi \left| \frac{\partial T}{\partial \Psi} (\Phi - \eta) \right| \frac{dF}{d\eta} \, d\eta \tag{A1}$$

The absolute value is to account for the heat addition being at either the upper or lower surface of the channel h_1 or h_2 in figure 3(a), that is, along $\widehat{78}$ or $\widehat{89}$. From the solution in reference 4 the response to a unit heat flux on one side of a slab of thickness h_n is

$$F(\Phi) = 2 \left(\frac{\Phi}{Pe}\right)^{1/2} \sum_{m=0}^{\infty} \left\{ \text{ierfc} \left[\frac{m h_n}{(\Phi/Pe)^{1/2}} \right] + \text{ierfc} \left[\frac{(m+1) h_n}{(\Phi/Pe)^{1/2}} \right] \right\} \tag{A2}$$

where the function ierfc ξ is defined as

$$\text{ierfc } \xi = \frac{1}{\sqrt{\pi}} e^{-\xi^2} - \xi \, \text{erfc } \xi$$

As shown by appendix B of reference 2, equation (A2) can be differentiated to obtain

$$\frac{dF}{d\Phi} = \left(\frac{1}{\pi \Phi Pe}\right)^{1/2} \sum_{m=0}^{\infty} \left[e^{-m^2 h_n^2 Pe/\Phi} + e^{-(m+1)^2 h_n^2 Pe/\Phi} \right] \tag{A3}$$

Substituting equation (A3) into equation (A1) yields the relation

$$T_w(\Phi) - T_\infty = \left(\frac{1}{\pi Pe}\right)^{1/2} \int_0^{\Phi} \left| \frac{\partial T}{\partial \Psi} (\Phi - \eta) \right| \frac{1}{\eta^{1/2}}$$

$$\times \sum_{m=0}^{\infty} \left[e^{-m^2 h_n^2 Pe/\eta} + e^{-(m+1)^2 h_n^2 Pe/\eta} \right] d\eta \tag{A4}$$

Case I $S/2b > 1.38$

As discussed in the ANALYSIS when $S/2b > 1.38$ $(0 < A \leq 1)$, equation (A4) has to be applied in two regions depending on whether X is greater or less than X_D. As shown in figure 3(a) for $S/2b > 1.38$ the heated region of the boundary starts at $\Phi = 0$ (point 8 in fig. 3(a)) and within this region $\left| \partial T/\partial \psi \right| = \left| 1/U \right|$. Hence equation (A4) becomes

$$T_w(\Phi) - T_\infty = \left(\frac{1}{\pi Pe}\right)^{1/2} \int_0^{\Phi} \frac{1}{\left| U(\Phi - \eta) \right|} \frac{1}{\eta^{1/2}}$$

$$\times \sum_{m=0}^{\infty} \left[e^{-m^2 h_n^2 Pe/\eta} + e^{-(m+1)^2 h_n^2 Pe/\eta} \right] d\eta \tag{A5}$$

Case II $S/2b < 1.38$

For this range figure 3(b) applies, and the heated portion of the boundary $\widehat{79}$ begins at $\Phi = \Phi_0$. Thus for any argument Φ', $\partial T/\partial \Psi(\Phi') = 0$ for $0 < \Phi' < \Phi_0$. Let the argument be $\Phi' = \Phi - \eta$. Then $\partial T/\partial \Psi(\Phi - \eta) = 0$ for $0 < \Phi - \eta < \Phi_0$ or for $\Phi > \eta > \Phi - \Phi_0$. Thus the integral in equation (A4) is zero for the range of η from $\Phi - \Phi_0$ to Φ and the remaining portion of the integral is for the range from $\eta = 0$ to $\Phi - \Phi_0$. The wall temperature distribution is then (U is positive in the region of integration so the absolute value sign is omitted)

$$T_w(\Phi) - T_\infty = \left(\frac{1}{\pi Pe}\right)^{1/2} \int_0^{\Phi-\Phi_0} \frac{1}{U(\Phi - \eta)} \frac{1}{\eta^{1/2}} \times \sum_{m=0}^{\infty} \left[e^{-m^2 h_n^2 Pe/\eta} + e^{-(m+1)^2 h_n^2 Pe/\eta} \right] d\eta \qquad \text{(A6)}$$

APPENDIX B

LIMITING VALUE AT $X = 0$ FOR $S/2b < 1.38$ ($-1 \leq A < 0$)

For spacings such that $S/2b < 1.38$, the two incident jets are beginning to merge into a single jet and the wall temperature at $X = 0$ is finite even with the neglect of axial conduction. The wall temperature distribution as a function of Φ is given by equation (31)

$$T_w(\Phi) - T_\infty = \left(\frac{1}{\pi Pe}\right)^{1/2} \int_0^{\Phi - \Phi_0} \frac{1}{U(\Phi - \eta)} \frac{1}{\eta^{1/2}} \times \sum_{m=0}^{\infty} \left[e^{-m^2 h_n^2 Pe/\eta} + e^{-(m+1)^2 h_n^2 Pe/\eta} \right] d\eta \qquad (B1)$$

From figure 3(b), the point 7 where $X = 0$ corresponds to $\Phi = \Phi_0$. Then for small X the upper limit in equation (B1) is very close to zero so that η is very small throughout the integration. For small η the exponents in equation (B1) are large negative numbers with the exception of the first exponential term which has a zero exponent when $m = 0$. Thus for very small η the summation approaches a value of unity and equation (B1) reduces to

$$T_w(\Phi) - T_\infty = \left(\frac{1}{\pi Pe}\right)^{1/2} \int_0^{\Phi - \Phi_0} \frac{1}{U(\Phi - \eta)} \frac{1}{\eta^{1/2}} d\eta \qquad (B2)$$

for $\Phi \to \Phi_0$ (that is as $X \to 0$).

From the mapping relation in equation (18), the location $X = 0$ corresponds to $\xi = 0$. Thus when evaluating equation (B2) for small X the values of ξ will be small. For small ξ, equation (16) becomes

$$U(\xi \to 0) = -A\xi^{1/2} \qquad (B3)$$

It is recalled that A is negative for this range of spacings so that U is positive.

The quantity Φ_0 corresponds to $X = 0$ where also $\xi = 0$. Hence from equation (19)

$$\Phi_0 = \frac{-(3 - A)}{2\pi} \ln \left| \frac{1}{1 - A} \right| - \frac{A + 1}{2\pi} \ln \left| \frac{1}{A + 1} \right| + \frac{1}{\pi} \ln \left| \frac{1}{A^2 + A(A^2 - 2A - 1) + 1} \right|$$

Thus

$$\Phi - \Phi_0 = \frac{-(3 - A)}{2\pi} \ln |1 - \xi| - \frac{(A + 1)}{2\pi} \ln |\xi + 1| + \frac{1}{\pi} \ln |\xi^2 + \xi(A^2 - 2A - 1) + 1| \tag{B4}$$

Using the series expansion of $\ln (1 + x) = x - \frac{x^2}{2} + \ldots$ valid for $x^2 < 1$ gives for small ξ,

$$\Phi - \Phi_0 = \frac{-(3 - A)}{2\pi} (-\xi) - \frac{(A + 1)}{2\pi} \xi + \frac{1}{\pi} \xi(A^2 - 2A - 1)$$

$$= \xi \frac{A}{\pi} (A - 3) \tag{B5}$$

Thus for small ξ,

$$\xi = \frac{\pi(\Phi - \Phi_0)}{A(A - 3)}$$

and it follows from equation (B3) that

$$U(\Phi) = -A \sqrt{\frac{\pi(\Phi - \Phi_0)}{A(A - 3)}} \quad \text{for } X \to 0 \tag{B6}$$

Equation (B6) is now substituted into equation (B2) to yield

$$T_w(X \to 0) - T_\infty = \left(\frac{1}{\pi Pe} \right)^{1/2} \int_0^{\Phi - \Phi_0} \frac{1}{-A} \sqrt{\frac{A(A - 3)}{\pi(\Phi - \eta - \Phi_0)}} \frac{1}{\eta^{1/2}} d\eta$$

Integrating gives

$$T_w(X \to 0) - T_\infty = \left[\frac{A(A-3)}{Pe}\right]^{1/2} \left(\frac{1}{-A\pi}\right) \left[2 \tan^{-1} \sqrt{\frac{\eta}{\Phi - \Phi_0 - \eta}}\right]_0^{\Phi-\Phi_0}$$

Noting that A is negative, this reduces to

$$T_w(X \to 0) - T_\infty = \left[\frac{A-3}{A\ Pe}\right]^{1/2} \tag{B7}$$

Equation (B7) is the desired result. The parameter A is related to the dimensionless spacing between the jet centerlines by means of equation (17).

APPENDIX C

ALTERNATE FORMULATION FOR LARGE X

At large x the flow that has turned along the plate has a uniform velocity (for the inviscid flow treated here) and has a width $2bh_2$ as shown in figure 5. The conditions at large x consist of a channel flow with uniform fluid velocity with one boundary insulated and the other boundary having a uniform heat addition along it. As discussed earlier, with conduction along the streamlines neglected, there is no energy transport across the dividing streamline. An overall energy balance can then be formed on the fluid flowing in the region bounded by the dividing streamline, the free streamline ψ_1, and the heated plate. The energy balance yields

$$q_w(x - x') = 2bh_2 v_\infty \rho C_p [\bar{t}(x) - t_\infty] \tag{C1}$$

where $x' = x_D$ for figure 5(a) and $x' = 0$ for figure 5(b). The $\bar{t}(x)$ is the integrated mean convective fluid temperature which for a uniform fluid velocity is equal to

$$\bar{t}(x) = \frac{1}{2bh_2} \int_0^{2bh_2} t(x, y)\, dy \tag{C2}$$

Since the wall heating q_w is specified, and the heated length $x - x'$ is known from the mapping solution of the flow configuration, the $\bar{t}(x)$ can be found from equation (C1). This fixes the average level of the temperature distribution, and it is then necessary to solve the energy equation to obtain the temperature distribution about this level. This distribution will provide the wall temperature variation along the plate.

The energy equation at large x where the fluid velocity is $|v_\infty|$ has the form

$$k\left(\frac{\partial^2 t}{\partial x^2} + \frac{\partial^2 t}{\partial y^2}\right) = |v_\infty| \rho C_p \frac{\partial t}{\partial x} \tag{C3}$$

From equation (C1) it is evident that with uniform heat addition along the plate, the mean fluid temperature rises linearly with x. At large x the temperature profile will become fully developed, that is, the shape of the profile about its mean value will not be changing with x. Using this behavior along with equation (C1) gives

$$\frac{\partial t}{\partial x} = \frac{\partial \bar{t}}{\partial x} = \frac{q_w}{2bh_2 |v_\infty| \rho C_p} \tag{C4}$$

Since all quantities on the right side are constants, $\partial^2 t/\partial x^2 = 0$. Substituting for $\partial t/\partial x$ and $\partial^2 t/\partial x^2$ into equation (C3) yields

$$k \frac{\partial^2 t}{\partial y^2} = \frac{q_w}{2bh_2} \tag{C5}$$

Integrate once and apply the condition that $\partial t/\partial y = 0$ at $y = 2bh_2$ to obtain,

$$k \frac{\partial t}{\partial y} = \frac{q_w}{2bh_2} (y - 2bh_2) \tag{C6}$$

Integrating again and taking into account the condition in equation (C4) yields

$$t = \frac{q_w}{2bh_2 k} \left(\frac{y^2}{2} - 2bh_2 y \right) + \frac{q_w x}{2bh_2 |v_\infty| \rho C_p} + C \tag{C7}$$

where C is a constant. Because a local heat balance along the wall was used, equation (C7) already satisfies the boundary condition $\left.\frac{\partial t}{\partial y}\right|_{y=0} = -\frac{q_w}{k}$.

The constant C has to be determined so that the solution will satisfy the mean temperature level $\bar{t}(x)$ as specified according to equation (C1). From equations (C2) and (C7),

$$\bar{t}(x) = \frac{1}{2bh_2} \int_0^{2bh_2} \left[\frac{q_w}{2bh_2 k} \left(\frac{y^2}{2} - 2bh_2 y \right) + \frac{q_w x}{2bh_2 |v_\infty| \rho C_p} + C \right] dy$$

$$\bar{t}(x) = -\frac{q_w}{3k} 2bh_2 + \frac{q_w x}{2bh_2 |v_\infty| \rho C_p} + C \tag{C8}$$

Substitute $\bar{t}(x)$ into equation (C1) and solve for C to obtain

$$C = \frac{q_w 2bh_2}{3k} - \frac{q_w x'}{2bh_2 |v_\infty| \rho C_p} + t_\infty \tag{C9}$$

Substitute C into equation (C7) to yield

$$t - t_\infty = \frac{q_w(x - x')}{2bh_2 |v_\infty| \rho C_p} + \frac{q_w}{2bh_2 k}\left(\frac{y^2}{2} - 2bh_2 y\right) + \frac{q_w 2bh_2}{3k} \tag{C10}$$

Evaluating at $y = 0$ to obtain the wall temperature distribution gives

$$t_w - t_\infty = \frac{q_w(x - x')}{2bh_2 |v_\infty| \rho C_p} + \frac{q_w 2bh_2}{3k} \tag{C11}$$

This becomes in dimensionless form

$$T_w - T_\infty = \frac{X - X'}{Pe\ h_2} + \frac{h_2}{3} \tag{C12}$$

which is the desired result for large X.

REFERENCES

1. Gedney, Richard T.; and Siegel, Robert: Inviscid Flow Analysis of Two Parallel Slot Jets Impinging Normally on a Surface. NASA TN D-4957, 1968.

2. Siegel, Robert: Analysis of Heat Transfer for a Normally Impinging Liquid-Metal Slot Jet. NASA TN D-7260, 1973.

3. Carslaw, Horatio S.; and Jaeger, J. C.: Conduction of Heat in Solids. Second ed., Oxford Univ. Press, 1959.

4. Siegel, Robert; and Goldstein, Marvin E.: Analytical Method for Steady State Heat Transfer in Two-Dimensional Porous Media. NASA TN D-5878, 1970.

5. von Kármán, Theodore; and Biot, Maurice A.: Mathematical Methods in Engineering. McGraw-Hill Book Co., Inc., 1940.

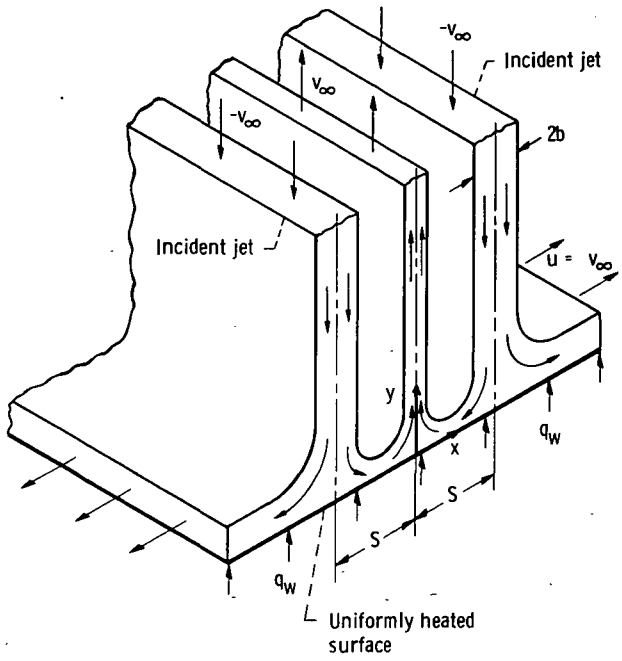

Figure 1. - Impingement of two liquid-metal slot jets against uniformly heated surface.

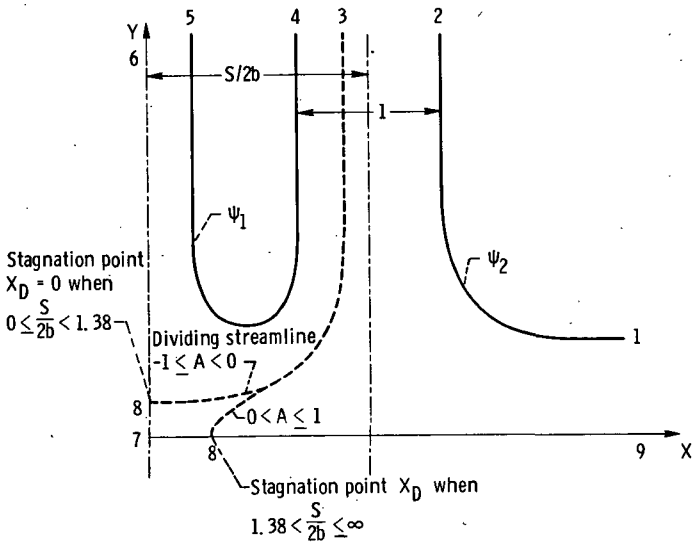

Figure 2. - Jet region in dimensionless physical plane.

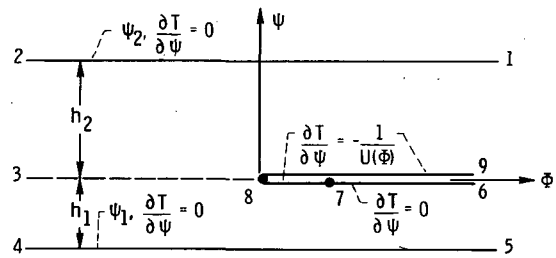

(a) Parameter, $0 < A \leq 1$.

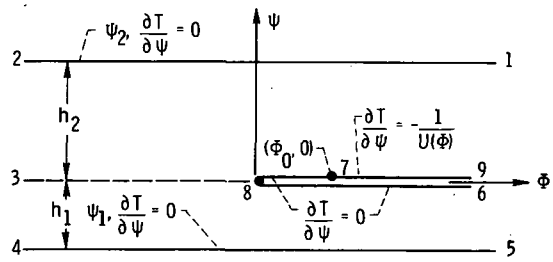

(b) Parameter, $-1 \leq A < 0$.

Figure 3. - Jet region and boundary conditions mapped into potential plane.

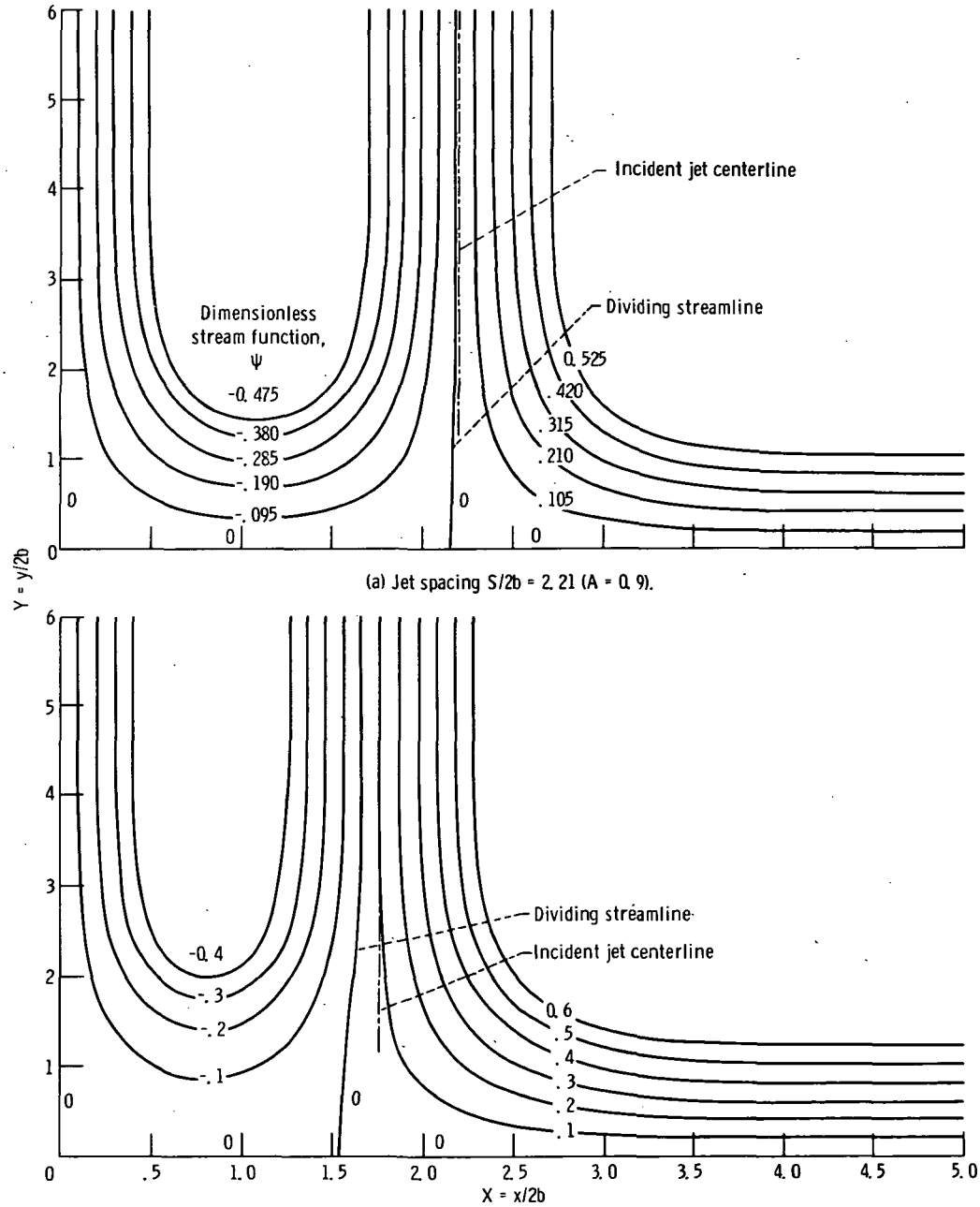

(a) Jet spacing S/2b = 2.21 (A = 0.9).

(b) Jet spacing S/2b = 1.78 (A = 0.6).

Figure 4. - Streamlines for two parallel slot jets impinging on a surface.

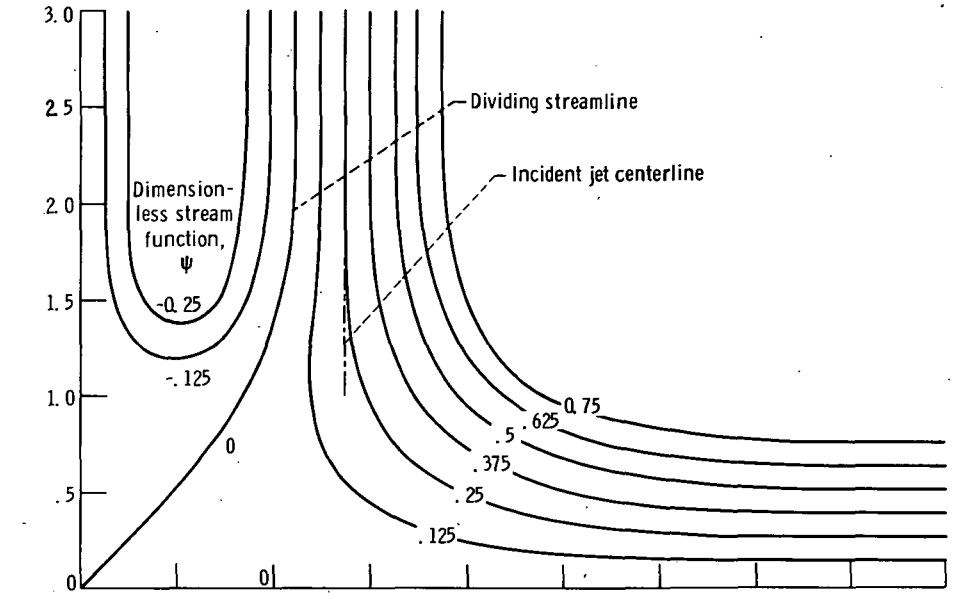

(c) Jet spacing S/2b = 1.38 (A = 0); configuration when all stagnation points coincide.

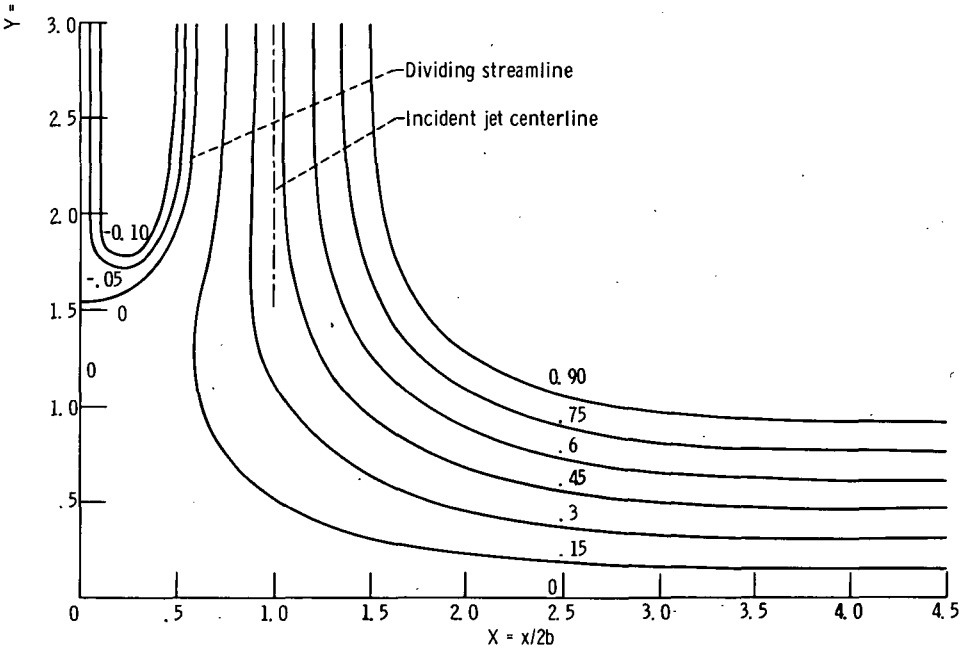

(d) Jet spacing S/2b = 1.00 (A = -0.6).

Figure 4. - Continued.

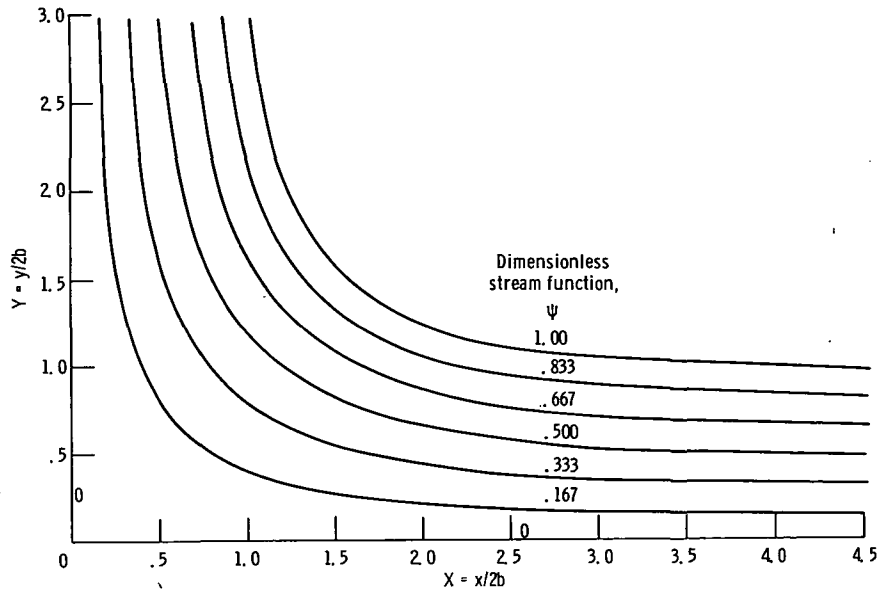

(e) Jet spacing S/2b = 0.5 (A = -1.0); two jets have merged to form single jet.

Figure 4. - Concluded.

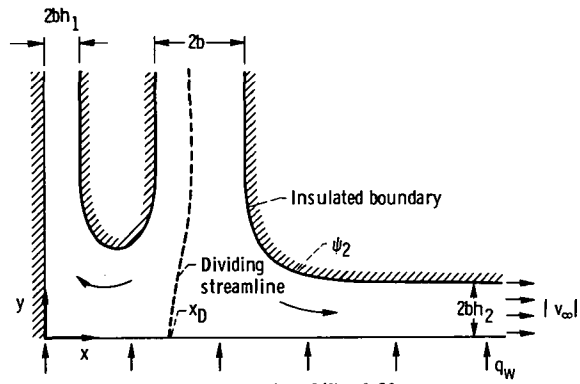

(a) Jet spacing S/2b > 1.38.

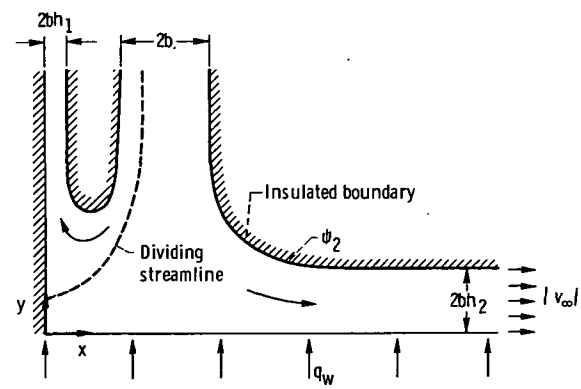

(b) Jet spacing S/2b < 1.38.

Figure 5. - Jet region in physical plane for analyzing conditions at large x.

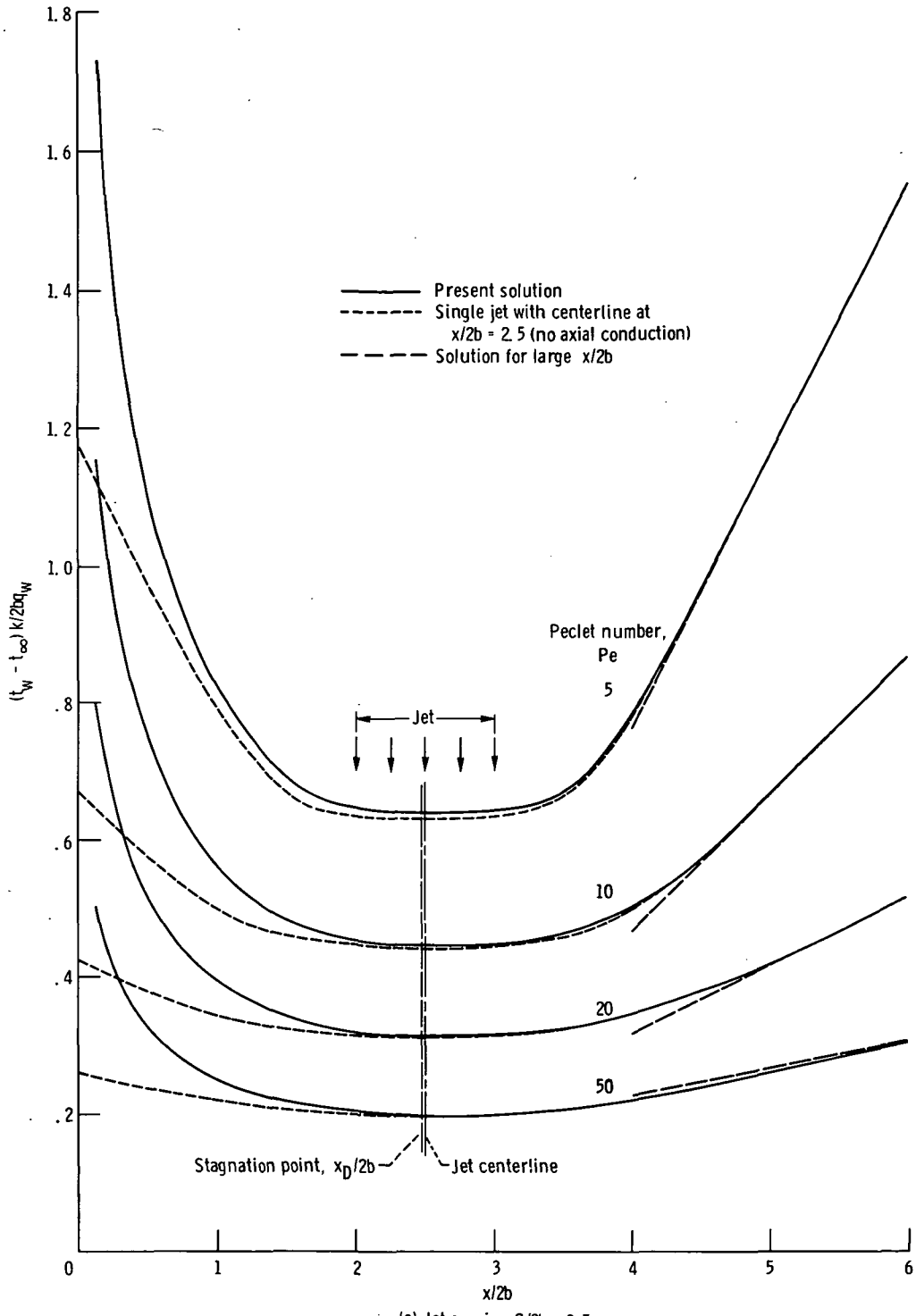

(a) Jet spacing S/2b = 2.5.

Figure 6. - Effect of jet Peclet number on dimensionless wall temperature variation for a fixed spacing between the incident jets.

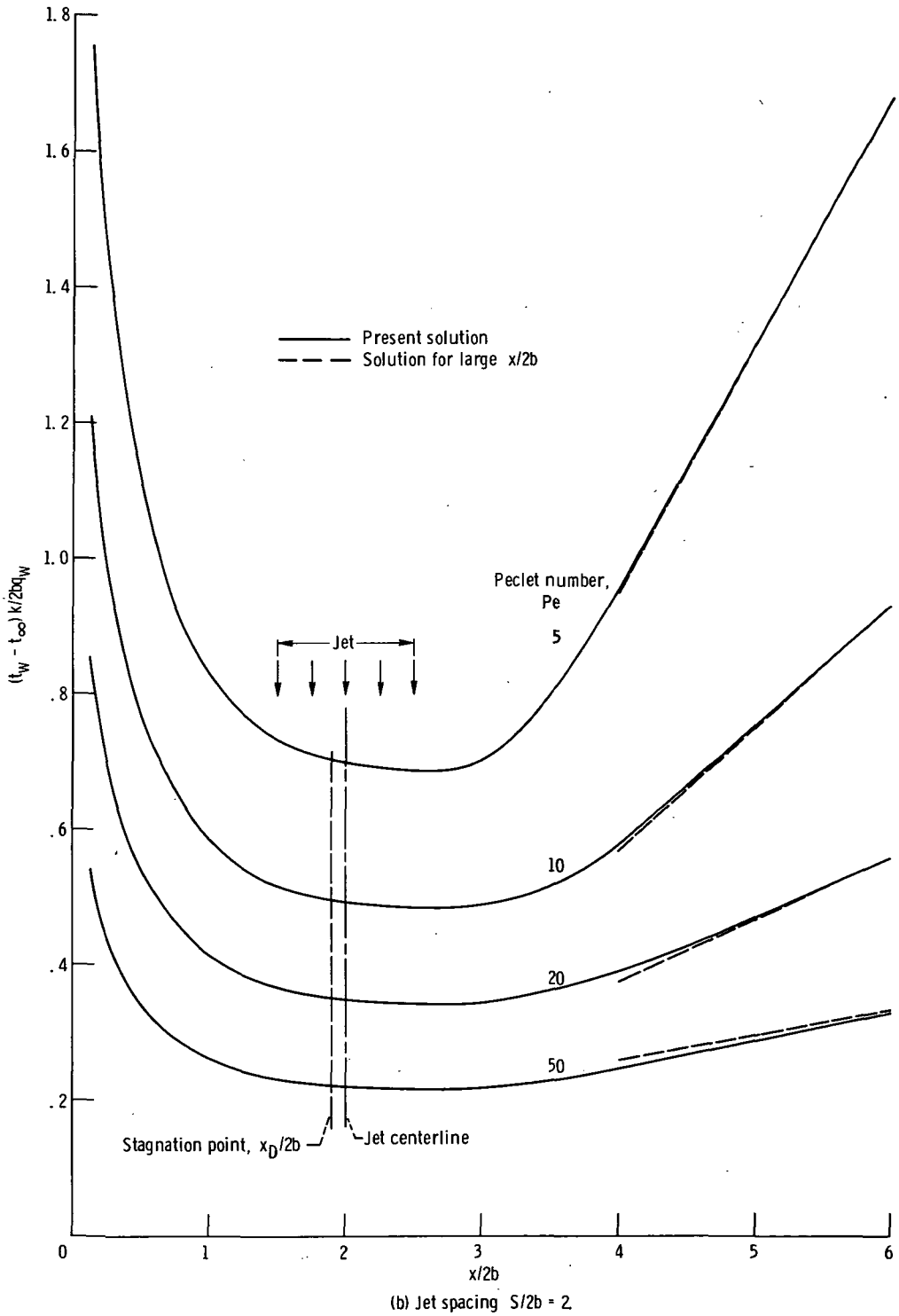

(b) Jet spacing S/2b = 2.

Figure 6. - Continued.

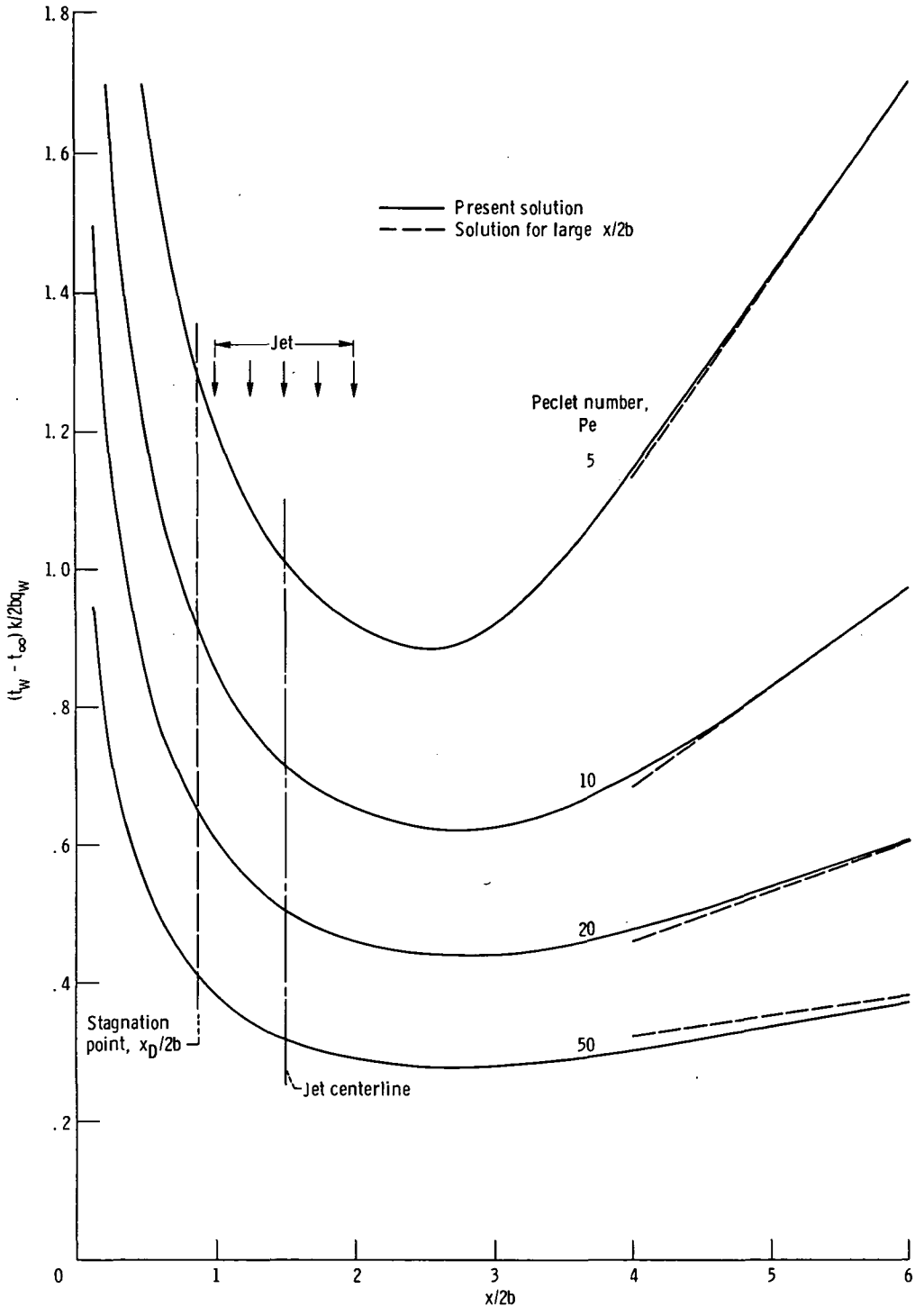

(c) Jet spacing S/2b = 1.5.

Figure 6. - Continued.

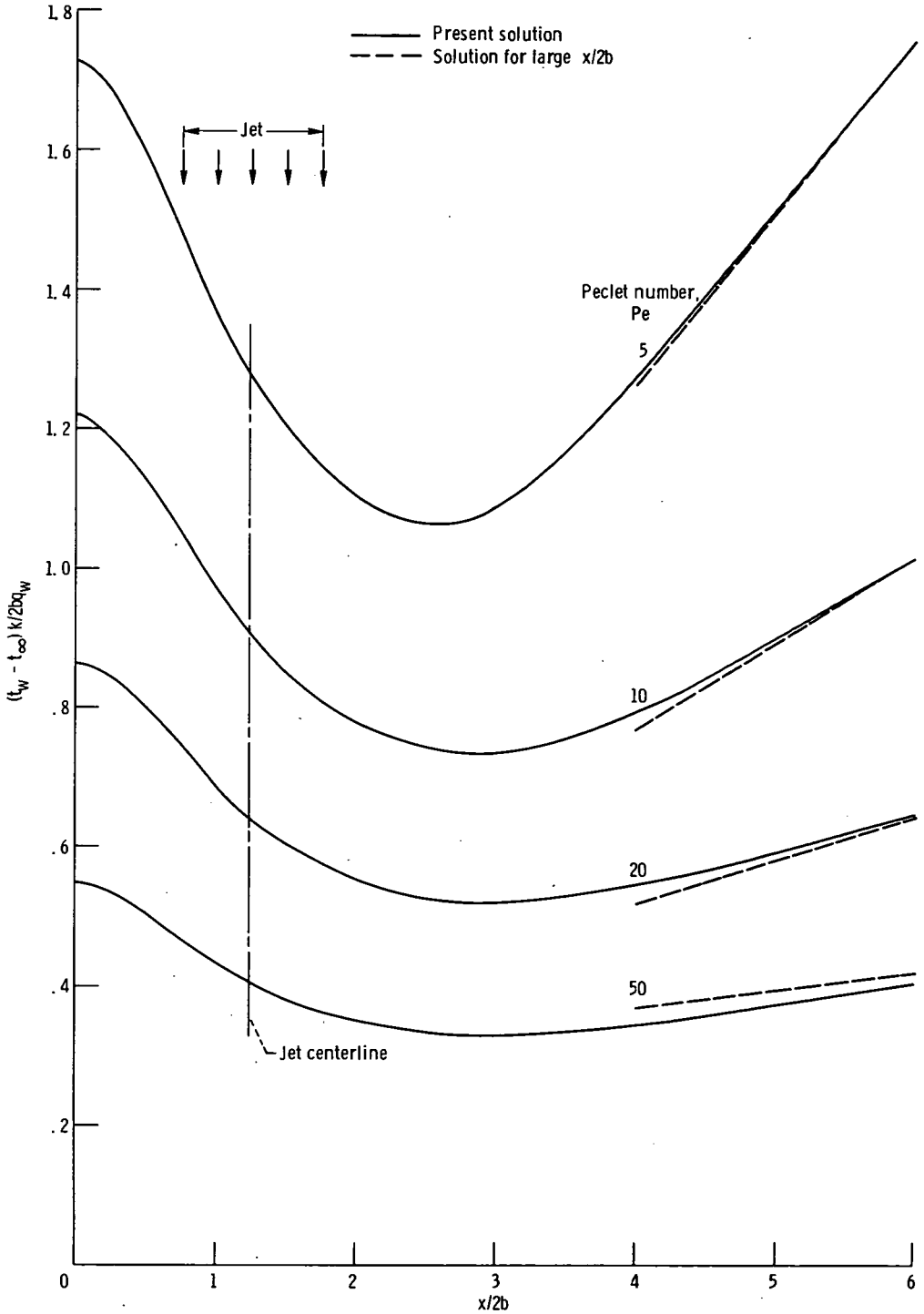

(d) Jet spacing S/2b = 1.25.

Figure 6. - Continued.

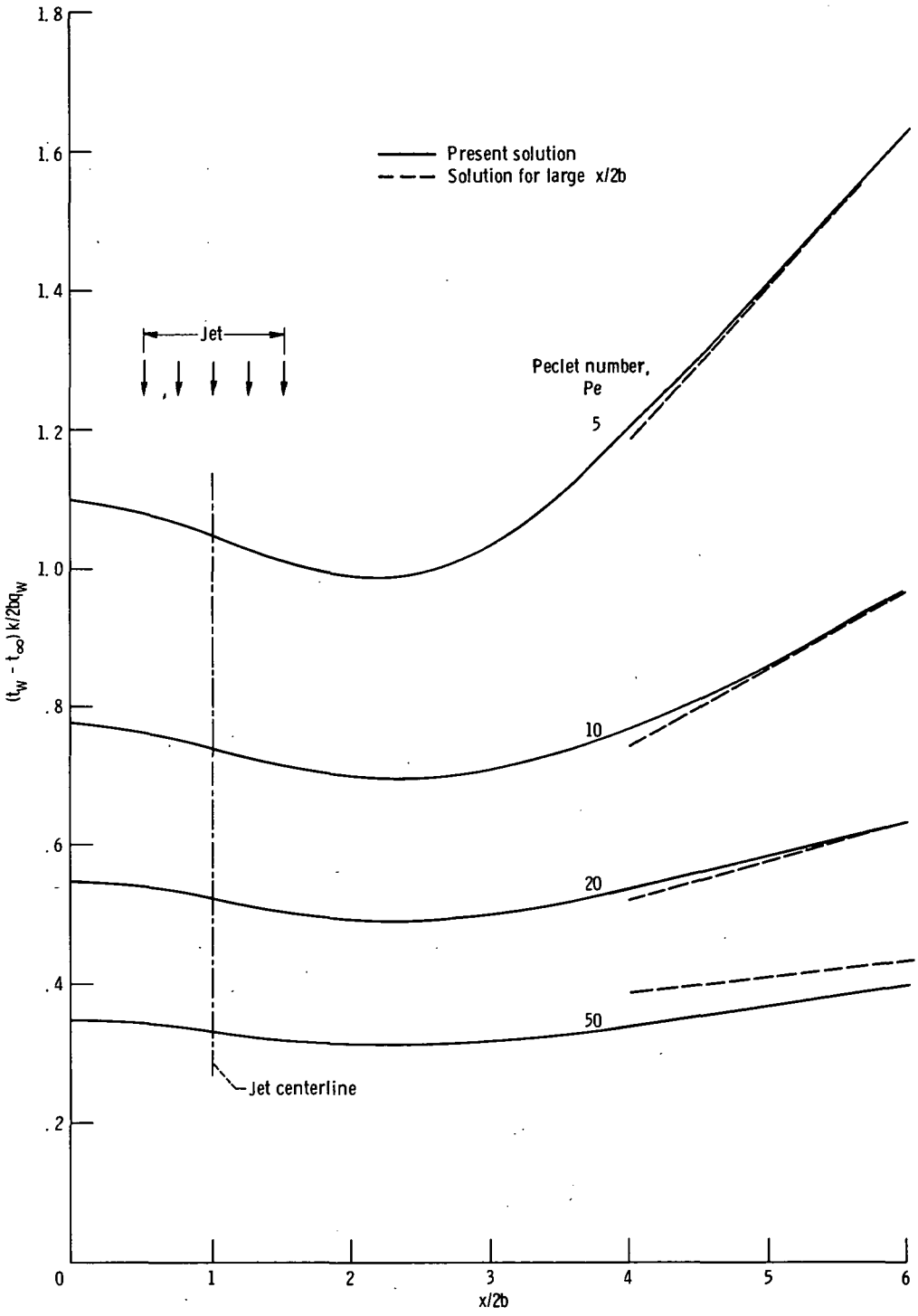

(e) Jet spacing S/2b = 1.0.

Figure 6. - Continued.

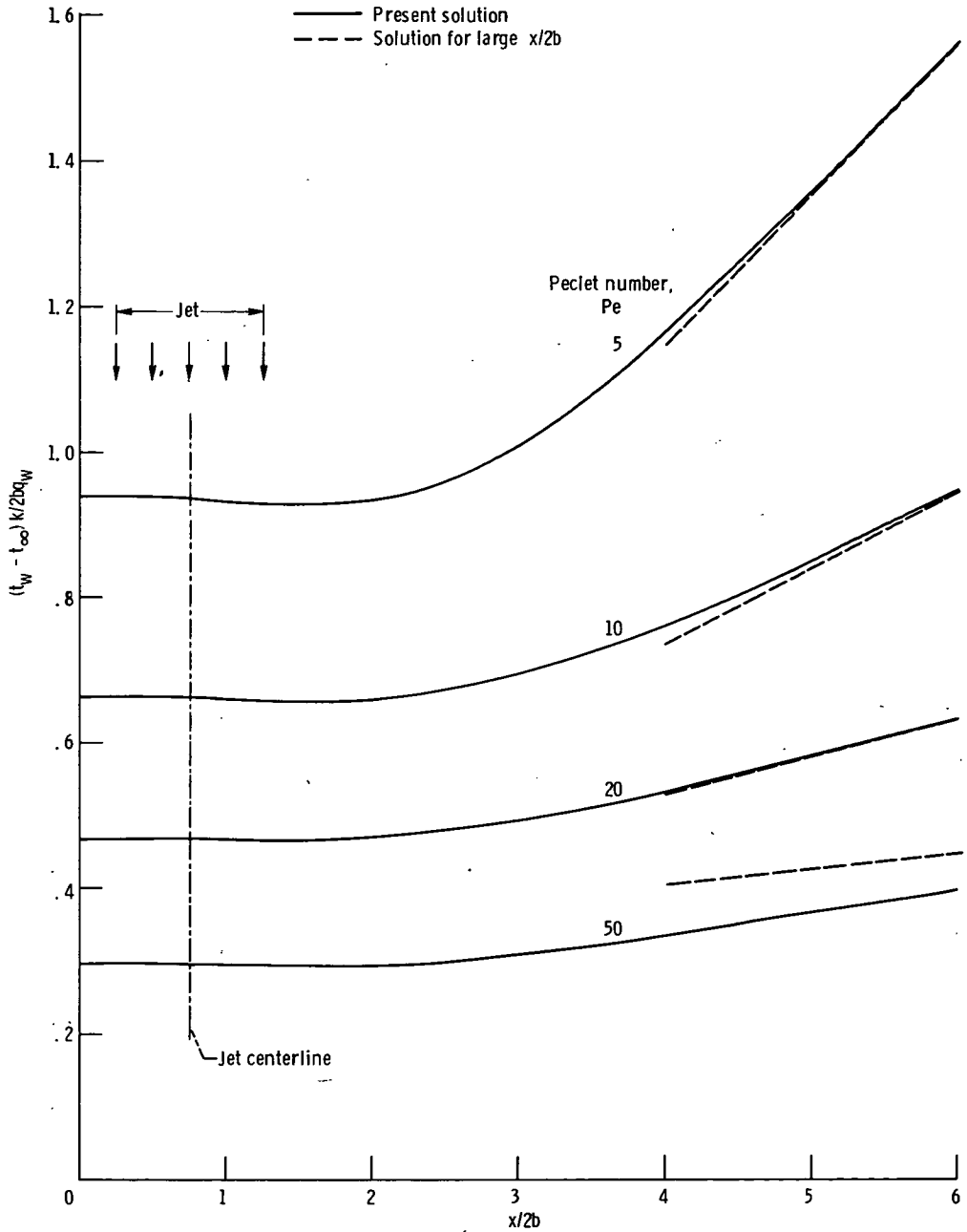

(f) Jet spacing S/2b = 0.75.

Figure 6. - Continued.

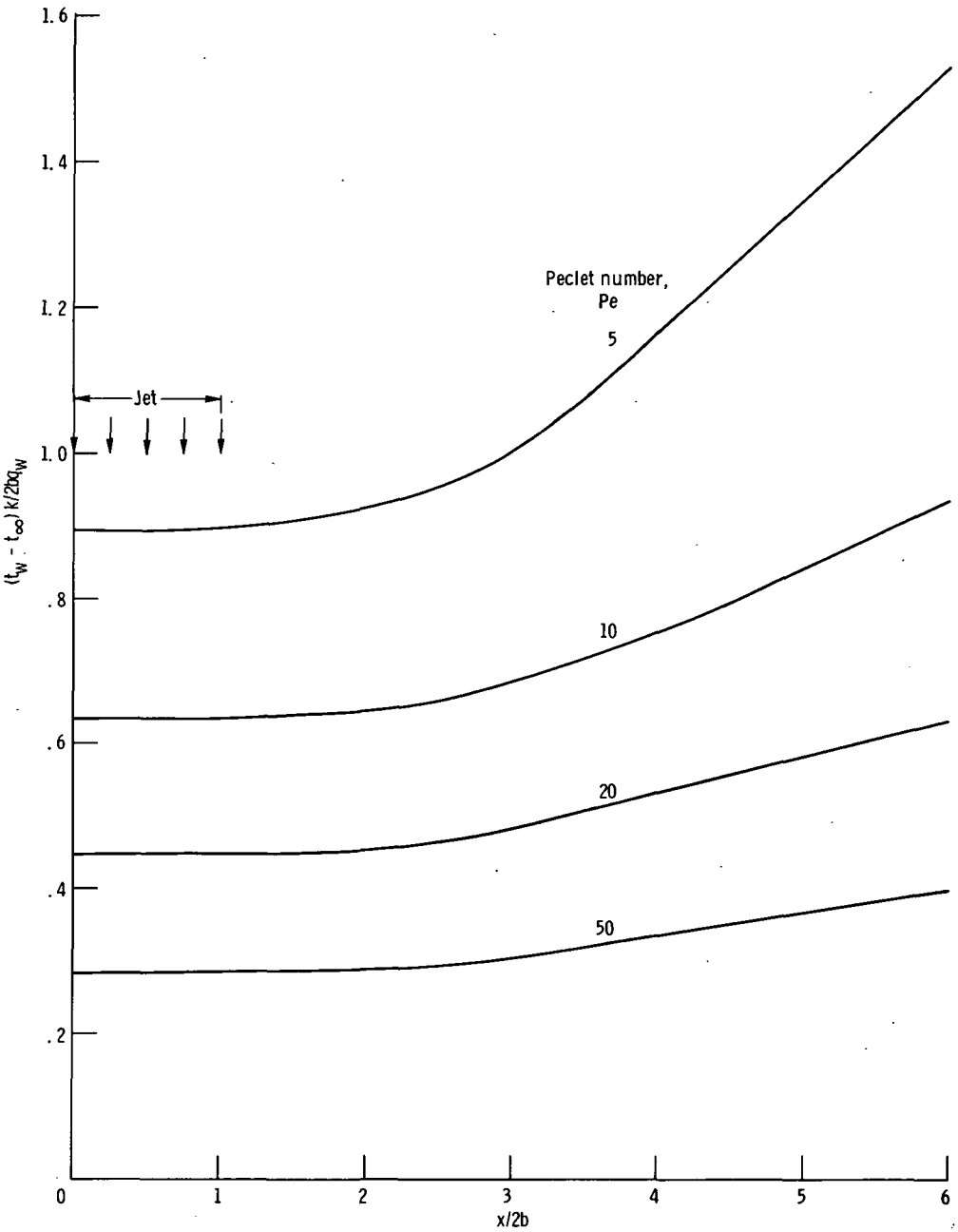

(g) Jet spacing S/2b = 0.5; two jets have merged into single jet of width 4b.

Figure 6. - Concluded.

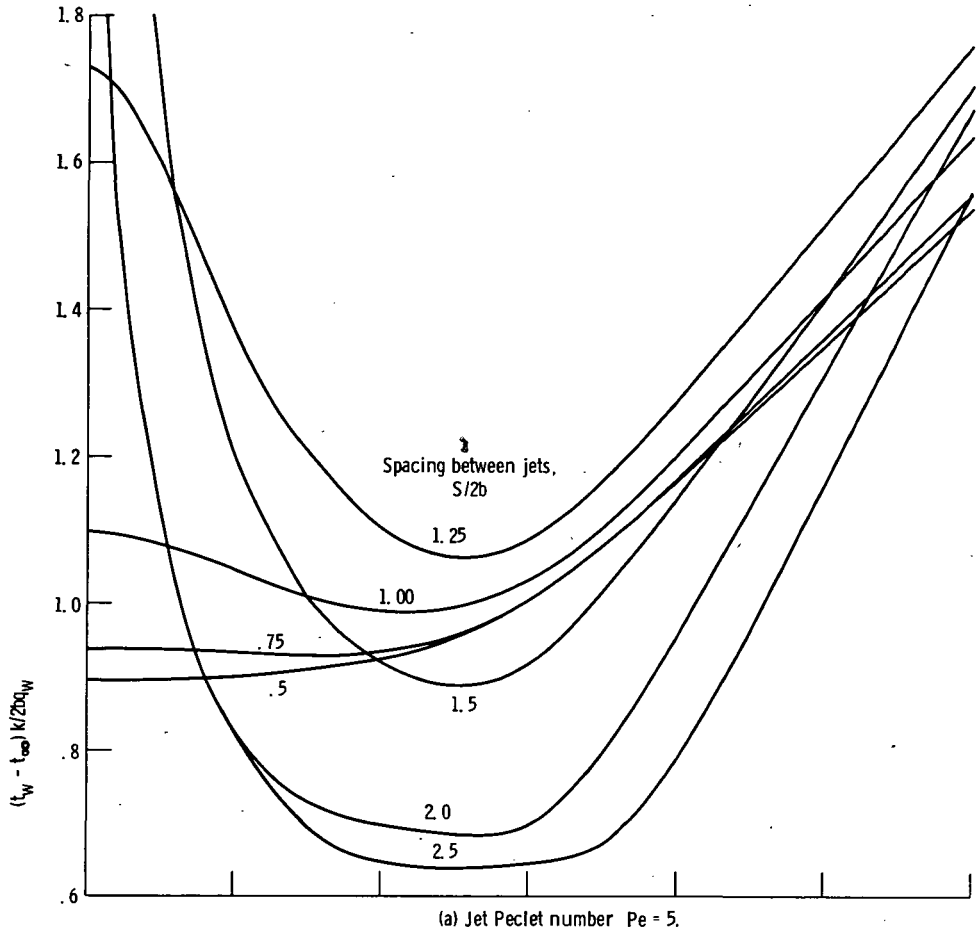

(a) Jet Peclet number Pe = 5.

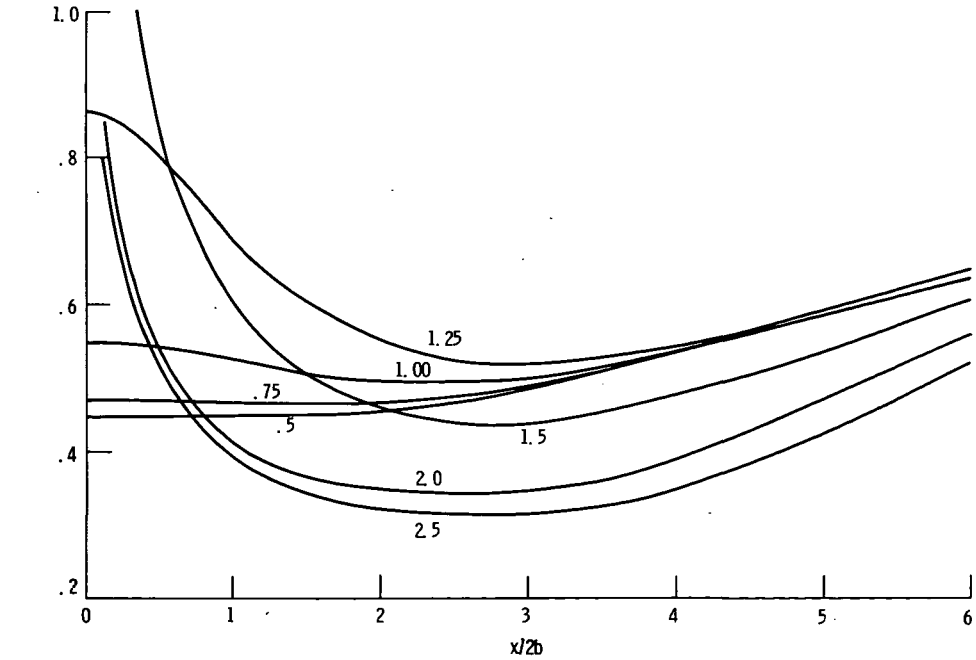

(b) Jet Peclet number Pe = 20.

Figure 7. - Effect of spacing between jets on dimensionless wall temperature variation for fixed Peclet number of incident jets.

"The aeronautical and space activities of the United States shall be conducted so as to contribute . . . to the expansion of human knowledge of phenomena in the atmosphere and space. The Administration shall provide for the widest practicable and appropriate dissemination of information concerning its activities and the results thereof."

—NATIONAL AERONAUTICS AND SPACE ACT OF 1958

NASA SCIENTIFIC AND TECHNICAL PUBLICATIONS

TECHNICAL REPORTS: Scientific and technical information considered important, complete, and a lasting contribution to existing knowledge.

TECHNICAL NOTES: Information less broad in scope but nevertheless of importance as a contribution to existing knowledge.

TECHNICAL MEMORANDUMS: Information receiving limited distribution because of preliminary data, security classification, or other reasons. Also includes conference proceedings with either limited or unlimited distribution.

CONTRACTOR REPORTS: Scientific and technical information generated under a NASA contract or grant and considered an important contribution to existing knowledge.

TECHNICAL TRANSLATIONS: Information published in a foreign language considered to merit NASA distribution in English.

SPECIAL PUBLICATIONS: Information derived from or of value to NASA activities. Publications include final reports of major projects, monographs, data compilations, handbooks, sourcebooks, and special bibliographies.

TECHNOLOGY UTILIZATION PUBLICATIONS: Information on technology used by NASA that may be of particular interest in commercial and other non-aerospace applications. Publications include Tech Briefs, Technology Utilization Reports and Technology Surveys.

Details on the availability of these publications may be obtained from:

SCIENTIFIC AND TECHNICAL INFORMATION OFFICE

NATIONAL AERONAUTICS AND SPACE ADMINISTRATION

Washington, D.C. 20546